IEEE Access
Multidisciplinary | Rapid Review | Open Access Journal

Received May 20, 2022, accepted June 3, 2022, date of publication June 8, 2022, date of current version June 13, 2022.

Digital Object Identifier 10.1109/ACCESS.2022.3181168

Statistically Thinned Array Antennas for Simultaneous Multibeam Applications

GIOVANNI BUONANNO[1], (Member, IEEE), SANDRA COSTANZO[1,3,4,5], (Senior Member, IEEE), AND RAFFAELE SOLIMENE[2,5,6], (Senior Member, IEEE)

[1]DIMES, University of Calabria, 87036 Rende, Italy
[2]Department of Engineering, University of Campania, 81031 Aversa, Italy
[3]Institute for Electromagnetic Sensing of the Environment (IREA), National Research Council (CNR), 80124 Naples, Italy
[4]National Inter-University Research Center on the Interactions between Electromagnetic Fields and Biosystems (ICEmB), 16145 Genoa, Italy
[5]National Inter-University Consortium for Telecommunications (CNIT), 43124 Parma, Italy
[6]Department of Electrical Engineering, Indian Institute of Technology Madras, Chennai 600036, India

Corresponding author: Giovanni Buonanno (giovanni.buonanno@unical.it)

ABSTRACT Statistically thinned array antennas are usually employed to form single-beam radiation patterns. In this work, the possibility to adopt such type of antennas to obtain multiple-beam patterns is successfully explored. In particular, two schemes are proposed and compared. In the first one, multiple-beam patterns are realized by considering each beam corresponding to a different feeding network. In the second scheme, multiple-beam behavior is achieved by a single feeding network. A key question addressed in this manuscript is given by the analysis of the statistical deviation of the synthesized radiation pattern, as compared to the reference one. To this end, the up-crossing method is employed. In particular, the assumption of symmetric thinned arrays leads to analytical results, but avoids the adoption of the simplified hypothesis which usually give inaccuracy. The proposed approach is verified by a Monte Carlo analysis, and shows very good agreement between empirical data and theoretical predictions.

INDEX TERMS Statistically thinned arrays, phased antenna arrays, nonuniformly-spaced arrays, density-tapered arrays, multi-beam applications.

I. INTRODUCTION

Statistically thinned arrays give a type of random array obtained by removing/turning off some elements from the so-called *reference filled* array, according to a probabilistic law which depends on the amplitude taper of the original reference array [1]–[4]. This type of array is appealing, as it requires a reduced number of elements (with respect to the reference array) to achieve the same resolution, with the peak side-lobe level mainly influenced by the residual elements after thinning operation. Moreover, no amplitude-tapering is needed, so that T/R modules can be used in their optimised configuration [1], [5]. Thinned arrays can be usefully adopted in a variety of applications, including satellite communications, radio-astronomy, ground-based high frequency radars, and interference cancellation by adaptive beam-forming. They can be generally adopted in all applications primarily requiring high resolution and low secondary lobes, rather than high gain [6]–[8]. They could be also exploited in the framework of mm-waves communications [9]–[11].

Thinning operation can be typically realized by the adoption of specific optimisation procedures [12]–[18]. In spite of better performance, these approaches generally entail a high computational cost, which can become cumbersome for large antenna arrays [8].

In this paper, statistically thinned arrays (STA) are considered. They are treated in terms of excitation coefficients typically given by binomial random variables. Other schemes assuming different levels for excitations have been also proposed in the literature [19]. Even if they provide a better approximation for the desired array factor, a more complicated feeding network is however required by this latter strategy.

The array factor of STA is a stochastic process which needs to be characterised by resorting to the probability theory. A statistical characterization is relatively easier in the

The associate editor coordinating the review of this manuscript and approving it for publication was Hussein Attia.

This work is licensed under a Creative Commons Attribution 4.0 License. For more information, see https://creativecommons.org/licenses/by/4.0/

presence of a high number of antenna elements, when the *Central Limit Theorem* (CLT) can be applied [3]. This is just the case where the reduction in the number of elements is more relevant. An accurate statistical characterization of a thinned array is generally difficult to obtain. Nonetheless, an *a priori* estimation of the array pattern (such as in terms of the peak side-lobe level) as a function of the array features and the thinning level, is highly desirable. To satisfy this need, several results have been produced over the years in literature, starting from the papers [1] and [3]. Recently, in [20], more accurate results have been presented for the case of *symmetric thinned arrays*. In particular, the up-crossing method has been used, but avoiding simplified assumptions which degrade the accuracy.

Statistically thinned arrays are generally adopted for single-beam applications, with possible linear phase excitation if a beam steering feature is required. However, many practical cases exist which impose the presence of simultaneous multiple beams [6]. Therefore, in this contribution, STA is applied to realize multiple-beam patterns. Two schemes are proposed. In the first one, each beam is associated to a different feeding network; hence, simultaneous independent beams can be obtained. The second scheme relies on a single feeding network, so the beams are no longer independent. In both cases, the approach developed in [20] is adopted to estimate the achievable performance in terms of two parameters, namely the array factor variance and the "distance" error between the statistical array factor and the reference one. The former is a local measure of the array factor dispersion around the reference array; the latter provides a "global" metric. In particular, by assuming symmetric STA, the mentioned performance parameters are obtained analytically, even if they account for the non-stationarity of the array factor, often neglected in other studies. Monte Carlo analysis is applied to successfully validate the theoretical predictions. Furthermore, we are dealing with the array factor only and no mutual coupling is assumed between antenna elements [21]. In any case, since thinned arrays are usually obtained from periodic lattices, they still allow a more adequate control of mutual coupling than aperiodic arrays. [4].

The work is organised as follows. Section II contains the fundamental concepts on single-beam statistically thinned arrays. In Section III, the two thinning schemes for multiple-beam array factors are outlined, while in section IV they are tested and validated by numerical analysis. Conclusions and potential future developments are finally reported. In addition, the paper includes an appendix section to support the theoretical derivations.

II. SYMMETRIC STATISTICALLY THINNED ARRAYS

For the sake of argument, we briefly report some basic concepts regarding statistically thinned arrays. Let us consider a linear array of N isotropic radiators arranged along the x axis within the segment $[-L/2, L/2]$, L being the array aperture in terms of wavelength (refer to Fig. 1). N is assumed to be even, and the elements are half-wavelength spaced at

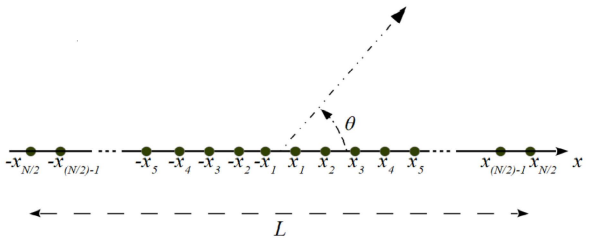

(a)

FIGURE 1. Geometry of a generic symmetric array.

$x_n = -x_{-n} = 0.25 + (n-1)0.5$, with $n = [1, 2, \ldots, N/2]$ (i.e., there is no element in the position $x = 0$). Moreover, the amplitude coefficients are chosen so that $A_{-n} = A_n$. The corresponding array factor can be written as

$$F_{ref}(u) = 2\sum_{n=1}^{N/2} A_n \cos[2\pi x_n(u-u_0)] \tag{1}$$

where $u = \cos\theta$ and $u_0 = \cos\theta_0$, with θ and θ_0 being the observation and the steering angles, respectively. Accordingly, the visible space is given by the interval $[-1, 1]$. $F_{ref}(u)$ is the so-called reference filled array factor, to be approximated by the thinned array.

Herein, we address the case of symmetric thinned arrays, which are obtained by thinning only half the array, and then, for each remaining element, by locating further elements in the position $-x_n$. The corresponding thinned array factor is given by [20]

$$F(u) = 2C\sum_{n=1}^{N/2} F_n \cos[2\pi x_n(u-u_0)] \tag{2}$$

where $\{F_n\}_{n=1}^{N/2}$ are independent Bernoulli random variables. In particular, $\mathcal{P}_r\{F_n = 1\} = 1 - \mathcal{P}_r\{F_n = 0\} = \overline{F_n} = p_n$ ($\mathcal{P}_r\{\cdot\}$ is a probability measure, while the term $\overline{F_n}$ represents the mean of F_n). Also, $0 \le p_n = \alpha A_n / \max_n\{A_n\} \le 1$, with $0 < \alpha \le 1$ being the *thinning factor*. Indeed, for $\alpha = 1$, natural thinning is obtained. $C = \max_n\{A_n\}/\alpha$. Note that, since an uniform arrangement has been considered, $F(u)$ is a periodic function.

Since the $\{F_n\}_{n=1}^{N/2}$ are random variables, $F(u)$ is a stochastic process whose mean and variance are respectively given as [20]

$$\mu(u) = F_{ref(u)} \tag{3}$$

$$\begin{aligned}\sigma^2(u) &= \overline{P(u)} - F_{ref}^2(u) \\ &= 4\sum_{n=1}^{N/2}\left(\max\{A_n\}A_n/\alpha - A_n^2\right)\cos^2[2\pi x_n(u-u_0)]\end{aligned} \tag{4}$$

where $P(u) = F^2(u)$ is the power-pattern of the (symmetric) thinned array, and $\overline{P(u)}$ gives its mean.

If the number N is sufficiently large, by virtue of the Lyapunov Central Limit Theorem [22], $F(u)$ is Gaussian (for each u), that is $F(u) \sim \mathcal{N}\left[F_{ref}(u), \sigma^2(u)\right]$. Furthermore, since $F(u)$ is periodic, $\mu(u)$ and $\sigma(u)$ are periodic as well [20]. Under these conditions, the cumulative distribution function (*cdf*) of the array factor magnitude (and consequently of the power-pattern) is easily found to be expressed as [20], [23], [24]

$$\mathcal{P}\{F(u) \le \xi\} = Q\left[-\frac{\xi + \mu_{\mathcal{S}}(u)}{\sigma_{\mathcal{S}}(u)}\right] - Q\left[\frac{\xi - \mu_{\mathcal{S}}(u)}{\sigma_{\mathcal{S}}(u)}\right] \quad (5)$$

in which $Q(x) = (1/\sqrt{2\pi}) \int_x^\infty e^{-x^2/2}\, dx$ [25]. It can be shown that eq. (5) can be written in a closed-form [23], by exploiting the condition that for positive arguments the Q-function can be written in a closed-form with very small errors [25].

The number of active elements $N_t = 2\sum_{n=1}^{N/2} F_n$ is a Gaussian random variable as well, with mean and variance equal to $(\alpha/\max\{A_n\})\,\mu(0)$ and $(\alpha/\max\{A_n\})^2\sigma^2(0)$, respectively [20].

It must be remarked that the above simple results are achieved due to the assumption of symmetric configurations. For general asymmetric arrays, the distribution of the array factor magnitude can be expressed in terms of a generalised non-central chi-square distribution with two degrees of freedom [26]. In this case, no closed-form can be obtained. Anyway, symmetric and asymmetric thinned arrays return the same mean array factor and the average of N_t. Furthermore, the difference in the achievable performance are not so relevant, as shown in [20].

III. MULTI-BEAMS STATISTICALLY THINNED ARRAYS

In this section, two schemes for obtaining a thinned array factor consisting of multiple beams are introduced. Basically, they are obtained by adapting the general statistical thinning approach outlined in the previous section. For convenience, such schemes are addressed in the sequel as *scheme 1* and *scheme 2*.

The starting point is the definition of the multiple-beam reference array factor

$$F_{ref_{\mathcal{M}}}(u) = \sum_{n=-N/2}^{N/2} A_n B_n e^{2j\pi x_n u} \quad (6)$$

with $B_n = \sum_{m=1}^{M} e^{-2j\pi x_n u_m}$. It is seen that $F_{ref}(u)$ consists of M identical beams which are steered at the directions u_m. Since $A_{-n} = A_n$ (and real) and $B_{-n} = B_n^*$, it is useful to arrange (6) as

$$F_{ref_{\mathcal{M}}}(u) = 2\sum_{n=1}^{N/2} \tilde{A}_n \cos(2\pi x_n u - \phi_n) \quad (7)$$

with $\tilde{A}_n = A_n|B_n|$ and $-\phi_n = \angle B_n$, or equivalently as

$$F_{ref_{\mathcal{M}}}(u) = 2\sum_{n=1}^{N/2} A_n\, [a_n \cos(2\pi x_n u) + b_n \sin(2\pi x_n u)] \quad (8)$$

with

$$a_n = \sum_{m=1}^{M} \cos(2\pi x_n u_m) \quad (9)$$

$$b_n = \sum_{m=1}^{M} \sin(2\pi x_n u_m) \quad (10)$$

A. SCHEME 1

By this scheme, thinning is achieved as follows

$$\begin{aligned} F_{\mathcal{M}_1}(u) &= \sum_{m=1}^{M} \left\{ 2C \sum_{n=1}^{N/2} F_n \cos[2\pi x_n (u - u_m)] \right\} \\ &= 2C \sum_{n=1}^{N/2} F_n\, [a_n \cos(2\pi x_n u) + b_n \sin(2\pi x_n u)] \end{aligned} \quad (11)$$

It is noted that by this scheme all the M beams share the same random coefficients $\{F_n\}_{n=1}^{N/2}$, which are the same as in (2). This means that the actual excitation coefficients pertaining to the multiple-beam reference array factor have not been employed in defining the binomial random variables and that, simply, all the beams are thinned in the same way. This scheme, however, allows to obtain independent steerable beams, in the sense that each beam can correspond to a different chain of phase shifters and therefore to a different signal [27]. Hence, this scheme can be exploited for simultaneous transmission of multiple signals.

The mean and variance of the above array factor are

$$\mu_{\mathcal{M}_1}(u) = F_{ref_{\mathcal{M}}}(u) \quad (12)$$

and (13), as shown at the bottom of the next page, with $P_{\mathcal{M}_1}(u)$ being the power-pattern related to scheme 1. According to the CLT, $F_{\mathcal{M}_1} \sim \mathcal{N}\left[F_{ref_{\mathcal{M}}}(u), \sigma^2_{\mathcal{M}_1}(u)\right]$. Moreover, the probability distribution of N_t is the same as the single-beam case. Therefore, by this thinning scheme, introducing additional beams does not change the distribution of the actual number of antenna elements that remains after the thinning. Finally, as in the classical single-beam case, the array factor "statistically" tends to the reference one when the number of elemental radiators increases.

B. SCHEME 2

In this case the multi-beam nature of the array factor is directly considered in thinning procedure. More in detail, the binomial random variables $\tilde{F}_n$ are now set according to the amplitude coefficients $\tilde{A}_n$ in (7), that is $\mathcal{P}_r\{\tilde{F}_n = 1\} = \tilde{F}_n = \tilde{p}_n = \alpha\,\tilde{A}_n/\max\{\tilde{A}_n\} = 1 - \mathcal{P}_r\{\tilde{F}_n = 0\}$. The resulting thinned array factor hence writes as

$$\tilde{F}_{\mathcal{M}_2}(u) = 2\tilde{C}\sum_{n=1}^{N/2} \tilde{F}_n \cos(2\pi x_n u - \phi_n) \quad (14)$$

in which $\tilde{C} = \max\{\tilde{A}_n\}/\alpha$.

This scheme can be obtained by feeding the antenna elements with a single chain of phase shifters, which

provide the N phases $\{\phi_n\}$. Therefore, while $M \times N_t$ phase shifters are needed for scheme 1, here, only $\widetilde{N}_t = 2\sum_{n=1}^{N/2} \tilde{F}_n$ phase shifters are required, with $\widetilde{N}_t$ being still a Gaussian random variable with mean $2\sum_{n=1}^{N/2} \tilde{p}_n$ and variance $4\sum_{n=1}^{N/2} \tilde{p}_n(1-\tilde{p}_n)$. Note that $\tilde{N}_t \neq N_t$. What is more, for scheme 2 the average number of active radiators depends on the number of beams. Also scheme 2 allows to obtain multi-beam array factors without amplitude tapering, though the excitation coefficients are different from the ones pertaining to scheme 1. However, by this scheme, the beams are not independent.

$F_{\mathcal{M}_2}(u)$ has again a Gaussian distribution with mean

$$\mu_{\mathcal{M}_2}(u) = F_{ref_{\mathcal{M}}}(u) \tag{15}$$

and variance

$$\begin{aligned}\sigma^2_{\mathcal{M}_2}(u) &= \overline{P_{\mathcal{M}_2}(u)} - F^2_{ref_{\mathcal{M}}}(u) \\ &= 4\sum_{n=1}^{N/2} A_n \left[\frac{\max\{\tilde{A}_n\}}{\alpha} - \tilde{A}_n\right] \cos^2(2\pi x_n u - \phi_n)\end{aligned} \tag{16}$$

C. GLOBAL CHARACTERISATION

A rough array factor characterization, and hence a comparison between the two schemes, can be given in terms of the distribution of the array factor magnitude, which, as remarked above, is easy to obtain for the symmetric case. However, the mean and variance of the array factor provides only local information, i.e., for each different value of u. A global metric, instead, should be linked to the *distance* (in a probabilistic sense) between the actual and the reference array factors. To this end, as in [20], we consider the normalised *standardised error*, $\epsilon(u) = [F_{\mathcal{M}_i}(u) - F_{ref_{\mathcal{M}}}(u)]/\sigma_{\mathcal{M}_i}(u)$ ($i = 1$ for scheme 1 and $i = 2$ for scheme 2). In particular, performance is estimated in terms of $\epsilon(u)$ magnitude supremum (with u implied)

$$\begin{aligned}&\mathcal{P}_r\left\{\mathcal{S} = \max_{u\in[-1,1]}\{|\epsilon|\} \leq \xi\right\} \\ &\quad = \mathcal{P}_r\left\{|F_{\mathcal{M}_i} - F_{ref_{\mathcal{M}}}| \leq \xi\, \sigma_{\mathcal{M}_i}\ \forall\, u \in [-1,1]\right\}\end{aligned} \tag{17}$$

By setting $\mathcal{H} = \max_{u\in[-1,1]}\{|F_{ref_{\mathcal{M}}}(u)|\}$, (17) is equivalently recast as

$$\begin{aligned}&\mathcal{P}_r\{\mathcal{S} \leq \xi\} \\ &\quad = \mathcal{P}_r\left\{\frac{|F_{\mathcal{M}_i} - F_{ref_{\mathcal{M}}}|}{\mathcal{H}} \leq \xi\, \frac{\sigma_{\mathcal{M}_i}}{\mathcal{H}},\ \forall\, u \in [-1,1]\right\}\end{aligned} \tag{18}$$

Equation (17) gives a measure of the error over the whole visible space, including the beam regions. Indeed, $\mathcal{P}_r\{\mathcal{S} \leq \xi\} = p\%$ entails that, with a probability of $p\%$, $\epsilon(u)$ lies between $F_{ref_{\mathcal{M}}}(u) - \xi\,\sigma_{\mathcal{M}_i}(u)$ and $F_{ref_{\mathcal{M}}}(u) + \xi\,\sigma_{\mathcal{M}_i}(u)$, for each u. In this sense, $F_{ref_{\mathcal{M}}}(u) - \xi\,\sigma_{\mathcal{M}_i}(u)$ and $F_{ref_{\mathcal{M}}}(u) + \xi\,\sigma_{\mathcal{M}_i}(u)$ can be considered as *generalised* p-percent level curves [20].

It can be verified that the magnitude of the coefficient of variation [28], $|CV(u)| = |\sigma_{\mathcal{M}_i}(u)/\mu_{\mathcal{M}_i}(u)|$, is relatively higher in the region of secondary lobes. Accordingly, it is expected that (18) is mainly contributed by the error in such a region, whereas $F_{\mathcal{M}_i}(u) \approx F_{ref_{\mathcal{M}}}(u)$ in correspondence of the main beams.

Finding a closed-form solution for the $\mathcal{S}$-distribution is a very complicated problem. However, for the symmetric thinned arrays under concern, the up-crossing method can be conveniently employed and it has proved to work remarkably well [24].

Let $\mathcal{N}_\xi$ be the number of times $|\epsilon(u)|$ up-crosses (*i.e.*, crosses with positive slope) the level ξ. Accordingly, a first result is $\mathcal{P}_r\{\mathcal{S} \leq \xi\} = 1 - \mathcal{P}_r\{\mathcal{N}_\xi \geq 1\} \geq 1 - \overline{\mathcal{N}_\xi}$ (assuming that $|\epsilon(u)|$ is below ξ at $u = -1$), where the Markov inequality, $\mathcal{P}_r\{\mathcal{N}_\xi \geq 1\} \leq \overline{\mathcal{N}_\xi}$ has been exploited and $\overline{\mathcal{N}_\xi}$ is the mean of the number of up-crossings. Hence, a lower bound for the $\mathcal{S}$-distribution is obtained. However, if $\mathcal{N}_\xi$ is modeled as a Poisson random variable [30], the $\mathcal{S}$-distribution as can be analytically estimated as [24]

$$\mathcal{P}_r\{\mathcal{S} \leq \xi\} \approx \mathcal{P}_r\{|\epsilon(-1)| \leq \xi\}\, e^{-\overline{\mathcal{N}_\xi}} \tag{19}$$

where $\mathcal{P}_r\{|\epsilon(-1)| \leq \xi\}$ can be calculated from (5). Here, the final crucial issue is the computation of $\overline{\mathcal{N}_\xi}$. This can be achieved as follows [22]

$$\overline{\mathcal{N}_\xi} = \int_{-1}^{1} du \int_0^\infty \gamma\, f_{|\epsilon||\epsilon|'}(\xi, \gamma; u)\, d\gamma \tag{20}$$

in which $f_{|\epsilon||\epsilon|'}(\xi, \gamma; u)$ is the joint probability density function of $|\epsilon(u)|$ and its first derivative. Since $\epsilon(u)$ is a real stochastic process, it follows that the determination of the up-crossings of $|\epsilon(u)|$ is equivalent to the simultaneous study of the up-crossings of $\epsilon(u)$ and $-\epsilon(u)$. Moreover, since $\epsilon(u)$ is a Gaussian process [3], then $\epsilon(u)$ and its derivative $\epsilon'(u) = d\epsilon(u)/du$ are jointly Gaussian [22] (of course, the same holds true for $-\epsilon(u)$ and its derivative). Eventually, (20) can be written as (see [20] for details)

$$\begin{aligned}\overline{\mathcal{N}_\xi} &= \frac{1}{\pi}\int_{-1}^{1} \sigma_{\epsilon'}(u)\, du \\ &= \frac{1}{\pi}\int_{-1}^{1} \sqrt{\frac{\sigma^2_{F'_{\mathcal{M}_i}}(u) - \{\sigma'_{\mathcal{M}_i}(u)\}^2}{\sigma^2_{\mathcal{M}_i}(u)}}\, du\end{aligned} \tag{21}$$

$$\begin{aligned}\sigma^2_{\mathcal{M}_1}(u) &= \overline{P_{\mathcal{M}_1}(u)} - F^2_{ref_{\mathcal{M}}}(u) \\ &= 4\sum_{n=1}^{N/2} \left\{\left[\frac{\max\{A_n\}}{\alpha} A_n - A_n^2\right] \times [a_n \cos(2\pi x_n u) + b_n \sin(2\pi x_n u)]^2\right\}\end{aligned} \tag{13}$$

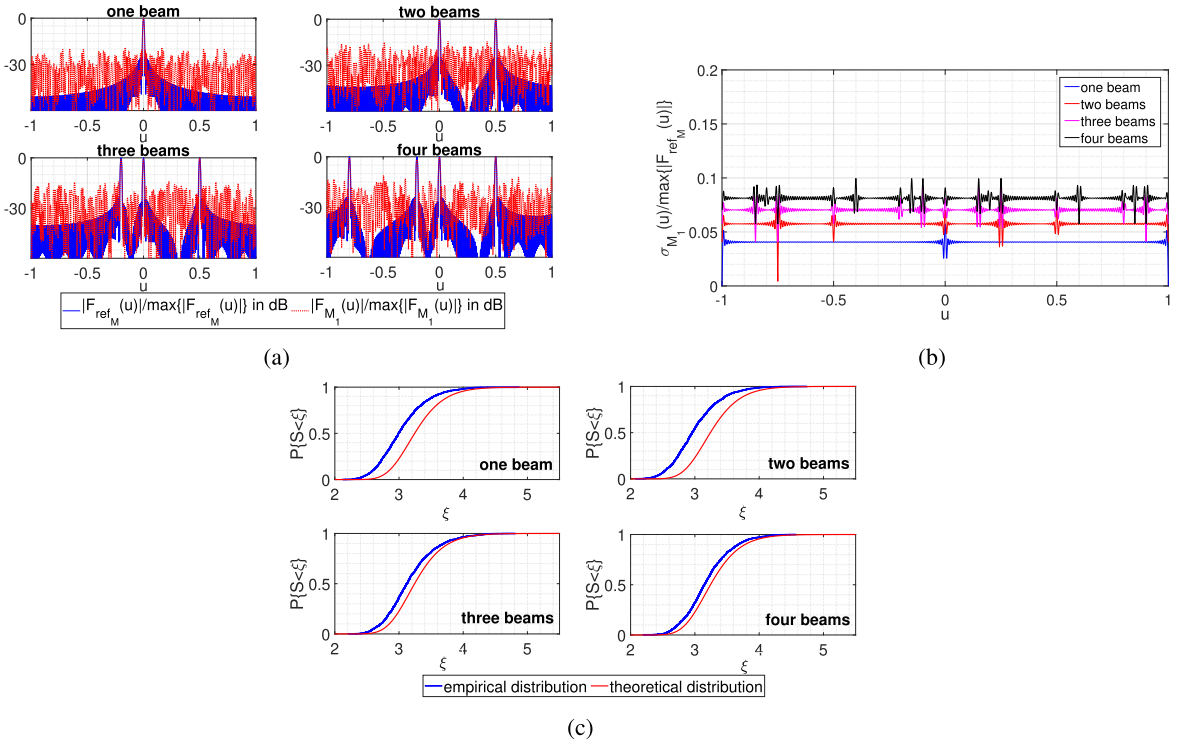

FIGURE 2. Performance analysis of scheme 1 for $N = 200$ and with $\approx 70\%$ of remaining elements (natural thinning $\Leftrightarrow \alpha = 1$), depending on the number of beams. (a) Magnitude of the reference array factor along with the magnitude of an array factor realisation. (b) Normalised standard deviation of the array factor. (c) $\mathcal{S}$-distributions.

in which $\sigma_{\epsilon'}(u)$ is the standard deviation of $\epsilon'(u)$, $\sigma_{F'_{\mathcal{M}_i}}(u)$ is the standard deviation of $dF_{\mathcal{M}_i}(u)/du$ (see Appendix), $\sigma'_{\mathcal{M}_i}(u) = d\sigma_{\mathcal{M}_i}(u)/du$. Note that in (21), we exploited the Bravais-Pearson correlation coefficient between $\epsilon(u)$ and its derivative is zero, for each u [20].

It is worth stressing once again the role of symmetric arrays assumption. As shown above, for the case at hand, $\mathcal{S}$-distribution can be accurately determined and is relatively simple to compute since only a one-dimensional integration is required to obtain $\overline{\mathcal{N}_\xi}$. Also, $\mathcal{P}_r\{|\epsilon(-1)| \leq \xi\}$ can be calculated in an extremely simple way. The same does not hold true for asymmetric thinned arrays. In fact, in this case, to get tractable expressions, the real and imaginary part of $\epsilon(u)$ and their derivatives are considered as being four independent stationary Gaussian processes, with the real and imaginary part of $\epsilon(u)$ (resp. the real and imaginary part of $\epsilon'(u)$) having the the same variance [31]. These are strong assumptions that generally lead to unreliable results [23].

IV. NUMERICAL ASSESSMENT

In this section, a numerical analysis is presented to check the theoretical findings and compare the proposed statistically thinned array schemes.

To this end, each realisation (sample function [22]) of the stochastic thinned array factor is obtained by employing a sample step in the variable u of $1/(10L)$, which is 5 times finer than the sampling step required by the bandwidth of the power pattern. In particular, 2000 realisations are employed in the following examples.

Each beam of the reference array factor is obtained by sampling a Taylor n-bar current distribution with $\overline{n} = 5$ and side-lobe level equal to -25 dB [21]. Thus, the coefficients $\{A_n\}$ are related to the samples of the corresponding current distribution [4]. Furthermore, as stated above, elemental radiators are half-wavelength spaced.

In order to check the behavior of statistically thinned arrays as the number of beams varies, we consider four reference array factors. The first one consists of a single (that is, $M = 1$) Taylor beam centered at $u = u_1 = 0$, for which

$$\begin{cases} a_n^{(1)} = 1 \\ b_n^{(1)} = 0 \end{cases} \tag{22}$$

This single-beam case can be considered as a kind of touchstone for the other cases. The second case concerns two Taylor beams pointing at $u_1 = 0$ and $u_2 = 0.5$, respectively, which corresponds to set

$$\begin{cases} a_n^{(2)} = 1 + \cos(2\pi x_n 0.5) \\ b_n^{(2)} = \sin(2\pi x_n 0.5) \end{cases} \tag{23}$$

The third reference array factor presents three Taylor beams at $u_1 = 0$, $u_2 = 0.5$ and $u_3 = -0.2$ and thus

$$\begin{cases} a_n^{(3)} = 1 + \cos(2\pi x_n 0.5) + \cos(2\pi x_n 0.2) \\ b_n^{(3)} = \sin(2\pi x_n 0.5) - \sin(2\pi x_n 0.2) \end{cases} \tag{24}$$

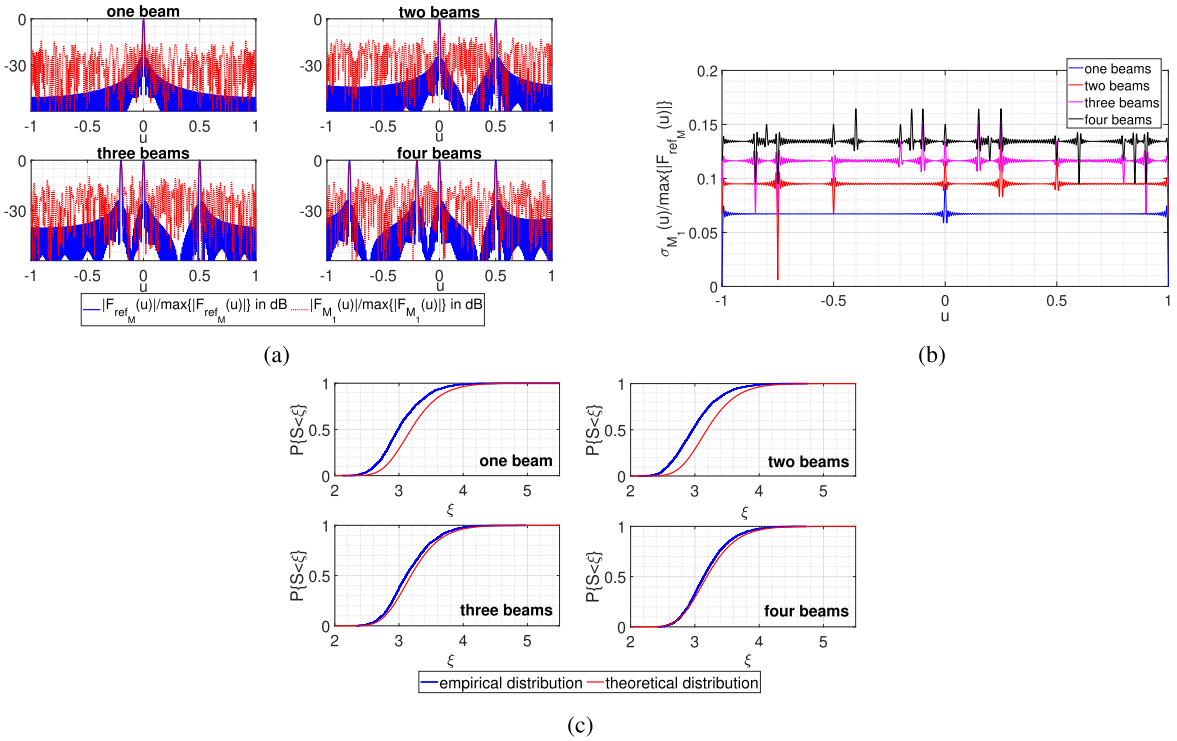

FIGURE 3. **Performance analysis of scheme 1 for $N = 200$ and with $\approx 50\%$ of remaining elements ($\alpha = 5/7$), depending on the number of beams. (a) Magnitude of the reference array factor along with the magnitude of an array factor realisation. (b) Normalised standard deviation of the array factor. (c) $\mathcal{S}$-distributions.**

and, finally, the last one has four Taylor beams at $u_1 = 0$, $u_2 = 0.5$, $u_3 = -0.2$ and $u_4 = -0.8$, thence with

$$\begin{cases} a_n^{(4)} = 1 + \cos(2\pi x_n 0.5) + \cos(2\pi x_n 0.2) + \cos(2\pi x_n 0.8) \\ b_n^{(4)} = \sin(2\pi x_n 0.5) - \sin(2\pi x_n 0.2) - \sin(2\pi x_n 0.8) \end{cases} \tag{25}$$

We would like to point out that here we just consider linear arrays for the sake of simplicity and for the computational burden purposes. However, the derived theoretical tools and the proposed thinned models can be easily generalised to deal with more general curved arrays. Also, they can be used for planar arrays while considering the cuts of the stochastic array factors, with a similar methodology as done in [1].

A. SCHEME 1

We consider three cases. Case 1 refers to $N = 200$ and $\alpha = 1$ (natural thinning), case 2 to $N = 200$ and $\alpha = 5/7$ (thinning at 50% percent) and case 3 to $N = 280$ and $\alpha = 5/7$ (average number of active elements equal to that of case 1). Although N may seem excessive for linear arrays, it is worth remarking that in the literature linear thinned arrays with elements till 2×10^4 [3] have been considered in order to study the properties of statistically thinned arrays.

Results concerning case 1 are shown Fig. 2. In this natural thinning case the average number of active elements is equal to 70% of the maximum number $N = 200$. Fig. 2a shows the magnitudes (in dB) for the four reference array factors discussed above and the magnitudes of realisations of thinned array factors, all normalised with respect to their supremum. As can be seen, the side-lobes of $|F(u)|/max\{|F(u)|\}$ increase with the number of beams. This trend was already observed for random aperiodic arrays [24], [29]. However, the main lobes of the actual and reference array factors are very similar. The above results are consistent with the variance behaviours reported in Fig. 2b. Indeed, as the number of beams increases, the variance levels become higher. This entails a greater dispersion around the actual reference array. Fig. 2c shows the comparison between the empirical and the theoretical $\mathcal{S}$-distributions (obtained by exploiting eq.(19)). As can be seen, those curves almost overlap and hence the theoretical estimation works very well.

It is interesting also to understand how the performance changes when the average of the actual number of elements, N_t, varies having fixed N or when the average of N_t is fixed and N increases. The next two examples just allow to shed some light on this question.

For case 2 a more severe thinning is imposed so that the average number of radiators after the thinning is lower than in the previous case. Indeed, now the mean of N_t is equal to 100, whereas in the previous case it was 140. Results concerning this case are reported in Fig. 3. As expected, previous considerations still apply. However, now the side-lobe level is in general increased; this is consistent with the variance behaviours that are higher than the corresponding previous cases. This basically confirms that the actual number of

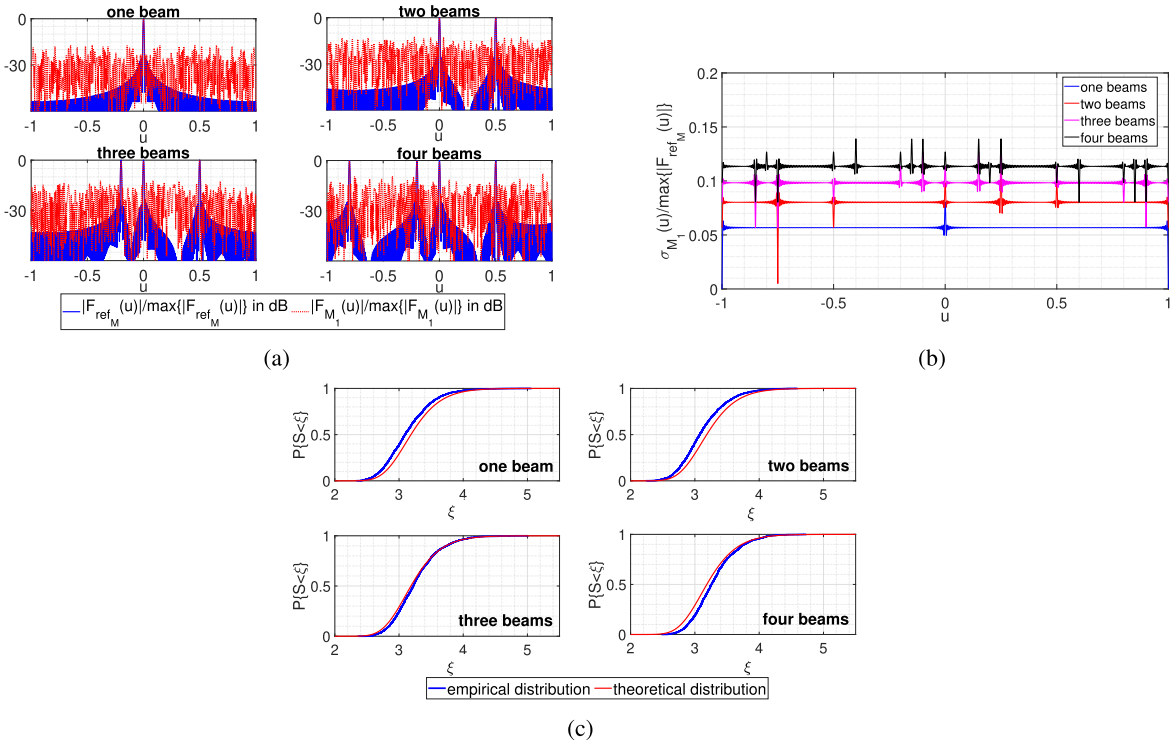

FIGURE 4. Performance analysis of scheme 1 for $N = 280$ and with $\approx 50\%$ of remaining elements ($\alpha = 5/7$), depending on the number of beams. (a) Magnitude of the reference array factor along with the magnitude of an array factor realisation. (b) Normalised standard deviation of the array factor. (c) $\mathcal{S}$-distributions.

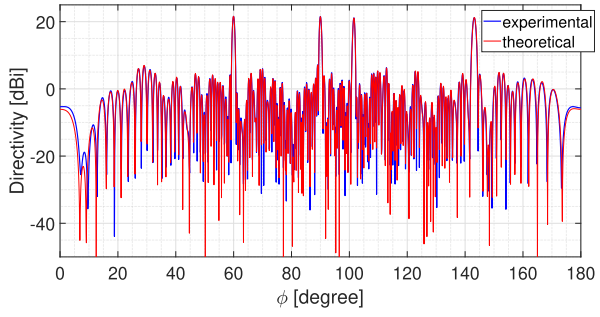

FIGURE 5. Scheme 1, four-beam case, $N = 200$, $\alpha = 1$. Experimental (blue line-CST simulation) and theoretical (red line) directivity, in the azimuth plane, of a statistically thinned linear array of cylindrical half-wavelength dipoles. Half wavelength spacing is considered between antenna elements. The dipoles are parallel to the z axis of the orthogonal Cartesian reference system, while the array axis coincides with the x axis. The operating frequency is equal to 1 GHz.

elements plays a crucial role in controlling the dispersion of the array factor realisations, [1], [20], [23]–[26]. The point is that such a dispersion can be precisely estimated through the analytical $\mathcal{S}$-distributions (see Fig. 3c).

In the last example (case 3), the maximum number of antenna elements is increased at $N = 280$, while the thinning is kept at 50%. This way, the mean of N_t is the same as case 1. Results are shown in Fig. 4. While the trend is of course the same as the previous cases, it is seen that the performance is in between the one of case 1 and 2 (see, for example, the variance behaviours in 4b). This entails that the achievable performance is not only affected by the average number of elements in the array (after the thinning), as it is often stated in the literature. However, our theoretical estimations of $\mathcal{S}$-distributions works remarkably well and hence gives a general tool to foresee the performance by accounting for all the relevant problem parameters.

As a further validation, scheme 1 was also tested using CST Studio Suite. In particular, Fig. 5 shows the comparison between the CST return and the theoretical directivity, in the azimuth plane, of a linear array of cylindrical half-wavelength dipoles arranged parallel to the z axis of the orthogonal Cartesian system, while the array axis coincides with the x axis. Moreover, $N = 200$, $\alpha = 1$, $M = 4$, the operating frequency is 1 GHz and the spacing between antenna elements is half a wavelength. As can be seen, an excellent matching is observed.

B. SCHEME 2

For the analysis of scheme 2, we consider two cases, $N = 200$ and $N = 280$, both under natural thinning conditions. Note that now, the average number of active radiators depends not only on α but also on the number of beams (in general, on the current distribution). Figs. 6 and 7 report the results for such cases. It is seen that, as N increases, the performance improves. As remarked above, this is a general trend that

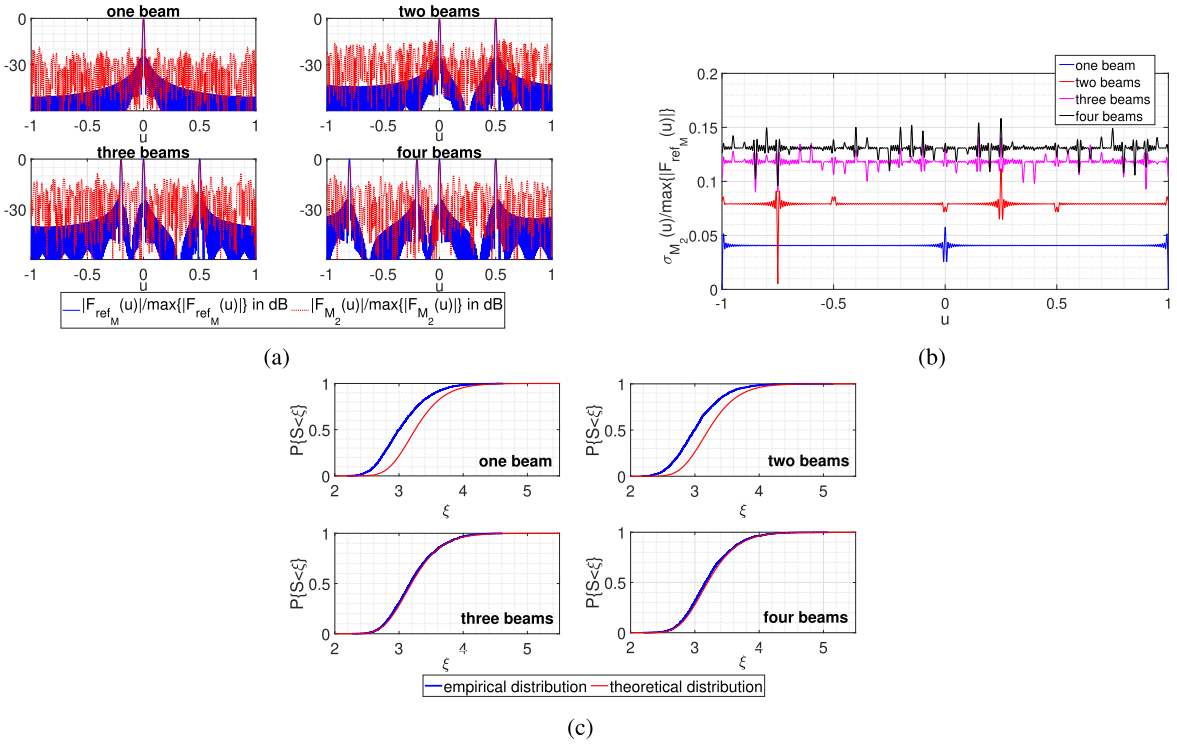

FIGURE 6. **Performance analysis of scheme 2 for $N = 200$ and in the natural thinning case ($\alpha = 1$), depending on the number of beams. (a) Magnitude of the reference array factor along with the magnitude of an array factor realisation. (b) Normalised standard deviation of the array factor. (c) $\mathcal{S}$-distributions.**

holds true also for scheme 2. However, with respect to scheme 1, by comparing Figs. 2 and 6, it is seen that a worsening occurs. Hence, scheme 1 is better but requires a more complex overall feeding network.

C. DISCUSSION

From previous results, it can be noted that the $\mathcal{S}$-distributions look nearly identical, regardless of the number of beams and the average number of retained elemental radiators. This, of course, does not mean that the distance between the statistically thinned array and the reference one is the same in all the cases. This is because $\mathcal{S}$-distributions refer to standardised processes. Indeed, what they actually measure is the probability that the array factor is globally within a strip (around the reference one) that depends on the standard deviation, $\sigma_{\mathcal{M}_i}(u)$, which in turn depends on the case under consideration. Also, as argued above, since the error is mainly related to the side-lobe regions, the $\mathcal{S}$-distribution gives an estimation of the peak level of secondary lobes.

Statistically thinned arrays are particularly suited for large antenna arrays which are populated by a high number of elements. In these cases, the statistical dispersion around the reference array factor can be made very low [3]. In this regard, we point out that, while the considered linear arrangement is chosen for computational convenience, the theory and the results can be easily adapted to deal with the one-dimensional cuts of a two-dimensional array factor.

Finally, in order to give a general picture of the achievable performance, the results shown above are summarized in Table 1. This table reports the rounded mean value of the number of active elements, $\overline{N_{t_i}}$, and the normalised standard deviation of the array factor, averaged over u, $\widetilde{\sigma_{\mathcal{M}_i}} = (1/2)\int_{-1}^{1}[\sigma_{\mathcal{M}_i}(u)/\max\{|F_{ref_{\mathcal{M}}}(u)|\}]\,du$ ($i = 1$ for scheme 1 and $i = 2$ for scheme 2). The addressed cases are distinguished by indicating (N, α). Looking at the table, the following conclusions can be drawn:

- For a given thinning factor, the variance decreases as the number of active elements increases;
- For a given average number of active elements, natural thinning performs better (compare $\widetilde{\sigma_{\mathcal{M}_1}}$ for the cases (200, 1) and (280, 5/7);
- While for scheme 1 the expected value of the number of active elements is always the same (regardless of the number of beams), this is not the case for scheme 2;
- With the same number of beams, N and α, scheme 1 is more efficient than scheme 2;
- $\widetilde{\sigma_{\mathcal{M}_i}}$ allows to roughly estimate the peak level of the secondary lobes.

Concerning the last point, consider, for example, the case in Fig. 2. Here, the highest level of the secondary lobes, for the (200, 1)-two beams sub-case (of scheme 1), is about -15 dB. Hence, the peak side lobe level is actually in between $2.5 \times \widetilde{\sigma_{\mathcal{M}_1}} = 2.5 \times 0.0574 \longrightarrow -16.86\,dB$ and $4 \times \widetilde{\sigma_{\mathcal{M}_1}} = 4 \times 0.0574 \longrightarrow -12.78$ dB (see Table 1 for the value of $\widetilde{\sigma_{\mathcal{M}_1}}$). Since $\mathcal{P}_r\{\mathcal{S} \leq 2.5\} \approx \epsilon$ (with ϵ being a very small

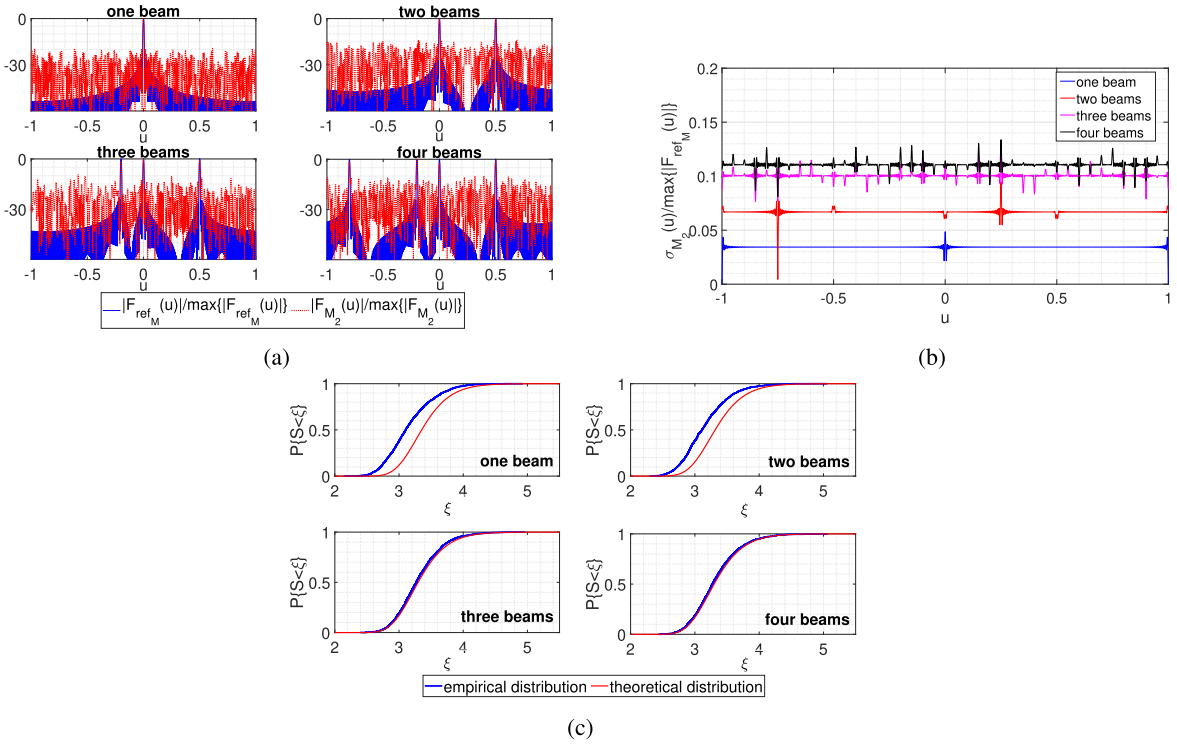

FIGURE 7. Performance analysis of scheme 2 for $N = 280$ and in the natural thinning case ($\alpha = 1$), depending on the number of beams. (a) Magnitude of the reference array factor along with the magnitude of an array factor realisation. (b) Normalised standard deviation of the array factor. (c) $\mathcal{S}$-distributions.

TABLE 1. (Rounded) expected value of active elements, $\overline{N_{t_i}}$, and mean value (with respect to u) of the normalised standard deviation of the array factor, $\widetilde{\sigma_{\mathcal{M}_i}}$, relative to the examples shown above ($i = 1$ for scheme 1, $i = 2$ for scheme 2). The vector (200, 1) means $N = 200$ and $\alpha = 1$ and the same holds for the other vectors. The acronym *n.b.* stands for number of beams.

	SCHEME 1								SCHEME 2					
	$(200,1)$		$(200,5/7)$		$(280,5/7)$		$(5000,1)$		$(200,1)$		$(280,1)$		$(5000,1)$	
$n.b.$	$\overline{N_{t_i}}$	$\widetilde{\sigma_{\mathcal{M}_1}}$	$\overline{N_{t_i}}$	$\widetilde{\sigma_{\mathcal{M}_1}}$	$\overline{N_{t_i}}$	$\widetilde{\sigma_{\mathcal{M}_1}}$	$\overline{N_{t_i}}$	$\widetilde{\sigma_{\mathcal{M}_1}}$	$\overline{N_{t_i}}$	$\widetilde{\sigma_{\mathcal{M}_2}}$	$\overline{N_{t_i}}$	$\widetilde{\sigma_{\mathcal{M}_2}}$	$\overline{N_{t_i}}$	$\widetilde{\sigma_{\mathcal{M}_2}}$
1	140	0.0406	100	0.0671	140	0.0567	3500	0.0081	140	0.0406	196	0.0343	3500	0.0081
2	140	0.0574	100	0.0949	140	0.0802	3500	0.0115	100	0.0791	139	0.0669	2475	0.0158
3	140	0.0703	100	0.1162	140	0.0983	3500	0.0141	81	0.1181	112	0.1004	1992	0.0239
4	140	0.0812	100	0.1342	140	0.1135	3500	0.0163	84	0.1309	118	0.1106	2103	0.0262

positive real number) and $\mathcal{P}_r\{\mathcal{S} \leq 4\} \approx 1$, 2.5×0.0574 and 4×0.0574 could be seen as the (statistical) minimum and maximum value of the highest level of the secondary lobes, respectively, if $\widetilde{\sigma_{\mathcal{M}_i}}$ can be considered nearly constant for $u \in [-1, 1]$. A more precise characterization can be obtained by considering lower and upper level curves, that is $\mathcal{LC}(u) = 2.5 \times [\sigma_{\mathcal{M}_i}(u)/\max\{|F_{DES_{\mathcal{M}}}(u)|\}]$ and $\mathcal{UC}(u) = 4 \times [\sigma_{\mathcal{M}_i}(u)/\max\{|F_{DES_{\mathcal{M}}}(u)|\}]$, that with probability almost equal to 1, contain the peak of secondary lobes for $u \in [-1, 1]$.

It is worth mentioning that Table 1 also reports cases with $N = 5000$, borrowed from [4], which clearly show that performance improves with the number of radiators.

V. CONCLUSION

Statistically thinned arrays have usually been studied for single-beam array factor, considering only a linear phase-shift for beam steering.

Here, we have introduced two statistically thinned array schemes for simultaneous multiple-beam generation. In particular, we have analytically characterized the achievable performance in terms of how the resulting array factor statistically deviates from the reference one. To this end, the array factor variance, which gives local information, and the supremum of the standardised error magnitude, which gives global information (i.e, over the whole visible space), have been derived and linked to the parameters of the problem, such as number of elements in the reference array, level of thinning, number of beams, etc.

The numerical analysis showed that increasing the number of beams leads to an increase of the distance between the thinned and the reference array factors. Whereas, performance improves as the number of active antenna elements increases. What is more, is that the theoretical findings are in excellent agreement with the outcome of the Monte Carlo numerical analysis. Hence, the obtained results

can be actually employed as a tool to set in advance the thinning strategy. In particular, the number of beams can be determined beforehand by checking if it is compatible with the desired performance.

APPENDIX A

For scheme 1, it is easy to prove that the mean of the derivative of the array factor, $F'_{\mathcal{M}_1}(u) = dF_{\mathcal{M}_1}(u)/du$, is $\mu_{F'_{\mathcal{M}_1}}(u) = \overline{dF_{\mathcal{M}_1}(u)/du} = dF_{ref_{\mathcal{M}}}(u)/du$, while the variance is

$$\begin{aligned}\sigma^2_{F'_{\mathcal{M}_1}}(u) &= \overline{\left[dF_{\mathcal{M}_1}(u)/du\right]^2} - \left[dF_{ref_{\mathcal{M}}}(u)/du\right]^2 \\ &= 16\pi^2 \sum_{n=1}^{N/2} \left\{ \left[\frac{\max\{A_n\}}{\alpha} A_n - A_n^2 \right] \right. \\ &\quad \left. \times \left[x_n b_n \cos(2\pi x_n u) - x_n a_n \sin(2\pi x_n u) \right]^2 \right\} \end{aligned} \tag{26}$$

For scheme 2, the mean of the derivative of the array factor, $F'_{\mathcal{M}_2}(u) = dF_{\mathcal{M}_2}(u)/du$, is also equal to $\mu_{F'_{\mathcal{M}_2}}(u) = dF_{ref_{\mathcal{M}}}(u)/du$ and the variance is

$$\begin{aligned}\sigma_{F'_{\mathcal{M}_2}}(u) &= \overline{\left[dF_{\mathcal{M}_2}(u)/du\right]^2} - \left[dF_{ref_{\mathcal{M}}}(u)/du\right]^2 \\ &= 16\,\pi^2 \sum_{n=1}^{N/2} \left[\frac{\max\{\tilde{A}_n\}}{\alpha} \tilde{A}_n - \tilde{A}_n^2 \right] \\ &\quad \times x_n^2 \sin^2(2\pi x_n u - \phi_n) \end{aligned} \tag{27}$$

REFERENCES

[1] M. I. Skolnik, J. Sherman, and F. Ogg, Jr., "Statistically designed density-tapered arrays," *IEEE Trans. Antennas Propag.*, vol. AP-12, no. 4, pp. 408–417, Jul. 1964.

[2] M. I. Skolnik, "Nonuniform arrays," in *Antenna Theory*, R. E. Collin and F. Zucker, Eds. New York, NY, USA: McGraw-Hill, 1969.

[3] Y. T. Lo, "Random periodic arrays," *Radio Sci.*, vol. 3, no. 5, pp. 425–436, May 1968.

[4] R. L. Haupt, *Antenna Arrays: A Computational Approach*. Hoboken, NJ, USA: Wiley, 2010.

[5] R. M. Leahy and B. D. Jeffs, "On the design of maximally sparse beamforming arrays," *IEEE Trans. Antennas Propag.*, vol. 39, no. 8, pp. 1178–1187, Aug. 1991.

[6] R. J. Mailloux, *Phased Array Antenna Handbook* (Artech House Antennas and Propagation Library), 2nd ed. Norwood, MA, USA: Artech House, 2005.

[7] R. L. Haupt, "Adaptively thinned arrays," *IEEE Trans. Antennas Propag.*, vol. 63, no. 4, pp. 1626–1632, Apr. 2015.

[8] F. Boulos, L. Dall'Asta, G. Gottardi, M. A. Hannan, A. Polo, A. Salas-Sanchez, and M. Salucci, "A computational inversion method for interference suppression in reconfigurable thinned ring arrays," *J. Phys., Conf. Ser.*, vol. 1476, no. 1, Mar. 2020, Art. no. 012016.

[9] H. Afzal, R. Abedi, R. Kananizadeh, P. Heydari, and O. Momeni, "An mm-wave scalable PLL-coupled array for phased-array applications in 65-nm CMOS," *IEEE Trans. Microw. Theory Techn.*, vol. 69, no. 2, pp. 1439–1452, Feb. 2021.

[10] Y. Yang, O. D. Gurbuz, and G. M. Rebeiz, "An eight-element 370–410-GHz phased-array transmitter in 45-nm CMOS SOI with peak EIRP of 8–8.5 dBm," *IEEE Trans. Microw. Theory Techn.*, vol. 64, no. 12, pp. 4241–4249, Dec. 2016.

[11] Y. Tousi and E. Afshari, "A scalable THz 2D phased array with +17 dBm of EIRP at 338 GHz in 65 nm bulk CMOS," in *IEEE Int. Solid-State Circuits Conf. (ISSCC) Dig. Tech. Papers*, Feb. 2014, pp. 258–259.

[12] R. L. Haupt, "Thinned arrays using genetic algorithms," *IEEE Trans. Antennas Propag.*, vol. 42, no. 7, pp. 993–999, Jul. 1994.

[13] N. Jin and Y. Rahmat-Samii, "Advances in particle swarm optimization for antenna designs: Real-number, binary, single-objective and multiobjective implementations," *IEEE Trans. Antennas Propag.*, vol. 55, no. 3, pp. 556–567, Mar. 2007.

[14] Z. He and G. Chen, "Synthesis of planar circular arrays with quantized amplitude weights," *Sensors*, vol. 21, no. 20, p. 6939, Oct. 2021.

[15] W. P. M. N. Keizer, "Large planar array thinning using iterative FFT techniques," *IEEE Trans. Antennas Propag.*, vol. 57, no. 10, pp. 3359–3362, Oct. 2009.

[16] W. P. M. N. Keizer, "Synthesis of thinned planar circular and square arrays using density tapering," *IEEE Trans. Antennas Propag.*, vol. 62, no. 4, pp. 1555–1563, Apr. 2014.

[17] X.-K. Wang, Y.-C. Jiao, and Y.-Y. Tan, "Synthesis of large thinned planar arrays using a modified iterative Fourier technique," *IEEE Trans. Antennas Propag.*, vol. 62, no. 4, pp. 1564–1571, Apr. 2014.

[18] E. Tohidi, M. M. Nayebi, and H. Behroozi, "Dynamic programming applied to large circular arrays thinning," *IEEE Trans. Antennas Propag.*, vol. 66, no. 8, pp. 4025–4033, Aug. 2018.

[19] R. J. Mailloux and E. Cohen, "Statistically thinned arrays with quantized element weights," *IEEE Trans. Antennas Propag.*, vol. 39, no. 4, pp. 436–447, Apr. 1991.

[20] G. Buonanno and R. Solimene, "Global characterization of linear statistically thinned antenna arrays," *IEEE Access*, vol. 9, pp. 119629–119640, 2021.

[21] C. A. Balanis, *Antenna Theory: Analysis and Design*, 2nd ed. New York, NY, USA: Wiley, 1996.

[22] H. Cramér and M. R. Leadbetter, *Stationary and Related Stochastic Processes: Sample Function Properties and their Applications*. New York, NY, USA: Dover, 2004.

[23] G. Buonanno and R. Solimene, "Large linear random symmetric arrays," *Prog. Electromagn. Res. M*, vol. 52, pp. 67–77, 2016.

[24] G. Buonanno and R. Solimene, "Unequally-excited linear totally random antenna arrays for multi-beam patterns," *IET Microw., Antennas Propag.*, vol. 12, no. 10, pp. 1671–1678, Aug. 2018.

[25] M. Zelen and N. C. Severo, "Probability functions," in *Handbook of Mathematical Functions With Formulas, Graphs and Mathematical Tables* (National Bureau of Standards Applied Mathematics Series), M. Abramowitz and I. A. Stegun, Eds. Jun. 1964.

[26] Y. T. Lo, "A mathematical theory of antenna arrays with randomly spaced elements," *IEEE Trans. Antennas Propag.*, vol. AP-12, no. 3, pp. 257–268, May 1964.

[27] M. I. Skolnik, *Introduction to Radar Systems*, 2nd ed. New York, NY, USA: McGraw-Hill, 1980.

[28] B. Everitt, *The Cambridge Dictionary of Statistics*. New York, NY, USA: Cambridge Univ. Press, 1998.

[29] G. Buonanno and R. Solimene, "Unequally excited generalised random binned antenna arrays," *IET Microw., Antennas Propag.*, vol. 13, no. 14, pp. 2531–2538, Nov. 2019.

[30] S. Krishnamurthy, D. W. Bliss, and V. Tarokh, "Sidelobe level distribution computation for antenna arrays with arbitrary element distributions," in *Proc. Conf. Rec. 45th Asilomar Conf. Signals, Syst. Comput. (ASILOMAR)*, Pacific Grove, CA, USA, Nov. 2011, pp. 6–9.

[31] M. Donvito and S. A. Kassam, "Characterization of the random array peak sidelobe," *IEEE Trans. Antennas Propag.*, vol. AP-27, no. 3, pp. 379–385, May 1979.

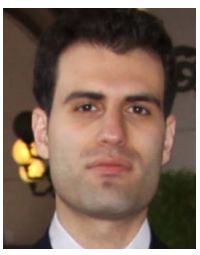

GIOVANNI BUONANNO (Member, IEEE) received the M.S. degree *(summa cum laude)* in electronic engineering from the Seconda Universita degli Studi di Napoli (SUN), Aversa, Italy, in 2014, and the Ph.D. degree in industrial and information engineering from the University of Campania "Luigi Vanvitelli," in 2018. Then, he joined the Research Group in Applied Electromagnetics, SUN. He is currently a Research Fellow with the University of Calabria. His research interests include analysis and design of nonuniformly-spaced antenna arrays, biomedical applications, and signal processing.

SANDRA COSTANZO (Senior Member, IEEE) received the Laurea degree *(summa cum laude)* in computer engineering from the Università della Calabria, Italy, in 1996, and the Ph.D. degree in electronic engineering from the Università Mediterranea di Reggio Calabria, Italy, in 2000. In 2017, she awarded the Italian National Scientific Qualification for the Full Professor position. Since 2019, she has been an Associate with IREA-CNR (Naples). She is currently an Associate Professor with the Università della Calabria, where she is the Co-ordinator of master's degree in telecommunication engineering and the Rector's Delegate for security, protection and control of electromagnetic fields. She teaches courses on electromagnetic waves propagation, antennas, remote sensing, radar, sensors, and electromagnetic diagnostics. She has authored or coauthored over 200 contributions in international journals, books, and conferences. Her research interests include near-field/far-field techniques, antenna measurement techniques, antenna analysis and synthesis, numerical methods in electromagnetics, millimeter wave antennas, reflectarrays, synthesis methods for microwave structures, electromagnetic characterization of materials, biomedical applications, and radar technologies. She is a member of the IEEE MTT-28 Biological Effects and Medical Applications Committee, the IEEE South Italy Geoscience and Remote Sensing Chapter, the Consorzio Nazionale Interuniversitario per le Telecomunicazioni (CNIT), the Società Italiana di Elettromagnetismo (SIEM), the Centro Interuniversitario sulle Interazioni fra Campi Elettromagnetici e Biosistemi (ICEMB), and a Board Member of the IEEE AP/ED/MTT North Italy Chapter. She received the Telecom Prize for the Best Laurea Thesis in 1996, and the Best Academia & Research Application in Aerospace and Defense 2013 Award for the Application Software Defined Radar using the NI USRP 2920 Platform. She is an Associate Editor of IEEE Access, the IEEE Journal of Electromagnetics, RF and Microwaves in Medicine and Biology, and *Electronics* (Section 'Microwave and Wireless Communications'), and an Editorial Board Member of *Radioengineering* and *International Journal of RF and Microwave Computer-Aided Engineering*. She is an Editor of the books *Microwave Materials Characterization* (INTECH, 2012) and *Wave Propagation Concepts for Near-Future Telecommunication Systems* (INTECH, 2017). She was the Lead Editor of Special Issues titled: *Reflectarray Antennas: Analysis and Synthesis Techniques* (2012), *Advances in Radar Technologies* (2013), *Compressed Sensing: Applications in Radar and Communications* (2016), *Bioengineering Applications of Electromagnetic Wave Propagation* (2019), and *Microwave Sensors for Biomedical Applications* (2020).

RAFFAELE SOLIMENE (Senior Member, IEEE) received the Laurea *(summa cum laude)* and Ph.D. degrees in electronic engineering from the Seconda Università degli Studi di Napoli (SUN), Aversa, Italy, in 1999 and 2003, respectively. In 2002, he became an Assistant Professor with the Faculty of Engineering, Mediterranea University of Reggio Calabria, Italy. Since 2006, he has been with the Dipartimento di Ingegneria, University of Campania "Luigi Vanvitelli," where he is currently an Associate Professor. Based on the following topics, he has coauthored more than 250 scientific works. His research interests include inverse electromagnetic problems with applications to inverse source and array diagnostics, non-destructive subsurface investigations, through-the-wall and GPR imaging, and breast cancer detection. On these topics, he routinely serves as a reviewer for a number of journals, and organized several scientific sessions. He is also an Associate Editor for four scientific journals, among which IEEE Geoscience and Remote Sensing Letters.